Intelligent Automation & Soft Computing
DOI:10.32604/iasc.2022.022380
Article

Error Calibration Model of Air Pressure Sensor Based on DF-RBF

Pengyu Liu[1,2,3,*], Wenjing Zhang[1,2,3], Tao Wang[1,2,3], Xiaowei Jia[4], Ying Ma[5], Kebin Jia[1,2,3] and Yanming Wang[1,2,3]

[1]Beijing University of Technology, Beijing, 100124, China
[2]Beijing Laboratory of Advanced Information Networks, Beijing, 100124, China
[3]Beijing Key Laboratory of Computational Inteligence and Inteligent System, Beijing, 100124, China
[4]Department of Computer Science, University of Pittsburgh, Pittsburgh, 15260, USA
[5]Qinghai Nationalities University School of Physics and Electronic Information Engineering, Qinghai, 810000, China
*Corresponding Author: Pengyu Liu. Email: liupengyu@bjut.edu.cn
Received: 05 August 2021; Accepted: 30 September 2021

Abstract: The development of upper-air meteorological detection is contingent upon the improvement of detection instruments. Air pressure sensors play a key role in high altitude meteorological measurement, but they can be frequently affected by temperature fluctutations, resulting in less accurate measurement data. The need to address this limitation has served as the core problem for meteorological detection and drawn great attention from the community. In this paper, we propose a calibration model for the DF-RBF air pressure sensor. The proposed method decomposes the detection process and corrects the measurements by fitting the residuals to true pressure values. In particular, we first calculate the error (*i.e.*, residual) between the measured pressure value and the true pressure values, and then build an analytical formula to represent the relationship between the measurement residual and the temperature. Then we decompose the function and fit its parameters through an RBF network. Finally, we generate the calibrated value by combining the measured value and the residual estimated by the analytical formula. In our experiments, we compare against a baseline method which predicts air pressure directly using temperature by fitting an RBF network. We observe that our proposed method, which combines sensor measurement and residual modeling, can achieve much lower measurement error (reduced from 1.5 to 0.7, over 53% error). This shows the feasibility and potential of the proposed method for barometric calibration.

Keywords: Sensor; calibration; nonlinear error correction; nonlinear fitting

1 Introduction

With the development of economy, science and technology, there is a growing interest from government and companies in studying climate change research and providing early warnings. The research along these directions require accurate and timely climate and weather information [1], which is often collected by meteorological sounding instrument. The barometric pressure sensor is a core component in meteorological sounding instrument, and is known to achieve good accuracy of measurement.

Theoretically, the air pressure sensor should have a linear relationship with its output air pressure. However, in practice, the air pressure sensor will be affected by fluctuating temperatures. There is a deviation between the real pressure and the measured pressure, the deviation in the air pressure value affects the accuracy of the final air pressure measurement [2]. Hence, there is an urgent need to improve air pressure measurement, which is critical for the development of meteorological research. In this paper, we aim to address the imperfection of such sensor data caused by temperature fluctuations.

Given the recent development of computer technology, there is a huge opportunity for using data-driven methods for calibrating high-altitude meteorological probe measuring instruments. In particular, Artificial Neural Network (ANN)-based methods have shown great promise to improve the accuracy of the software Calibration methods [3,4]. However, these data-driven methods commonly require a large set of training data while also ignoring the available information from air pressure measurement. To overcome such limitations, we leverage the data measured by air pressure sensors and then fix its bias given temperature fluctuations. First, we analyze the scatter graph distribution between the measured pressure and the standard pressure, and then we construct the analytic expression of the function between the error and the temperature. Third, we decompose the parameters of the analytic expression, and then combine the RBF network to obtain the complete analytic expression, and calculate the error value and the calibrated pressure value [5]. Finally, we complete the accurate calibration of the measured pressure. By decomposing the calibration process and fitting the residual (*i.e.*, the error), our method has considerably reduced the need for large training set, and also reduced the fitting time. Besides, it provides improved measurement accuracy for high-altitude weather detection.

2 Materials and Methods

2.1 The Principle Block Diagram of Air Pressure Sensor Error Correction

The air pressure sensor used in this study is a novel M- pressure sensor, with an allowable temperature range [–30°C, 30°C] , and the pressure range [5 hPa, 1100 hPa]. The characteristic curve between the calibration temperature point and the original output pressure value is shown in Fig. 1. In this Figure, the original pressure value is the undeciphered measured pressure value, which is only used to highlight the characteristic changes of the pressure sensor. It can be clearly seen that the change trend at different temperature points is biased. To solve this problem, we aim to build a calibration model of the air pressure sensor to eliminate the error caused by temperature changes.

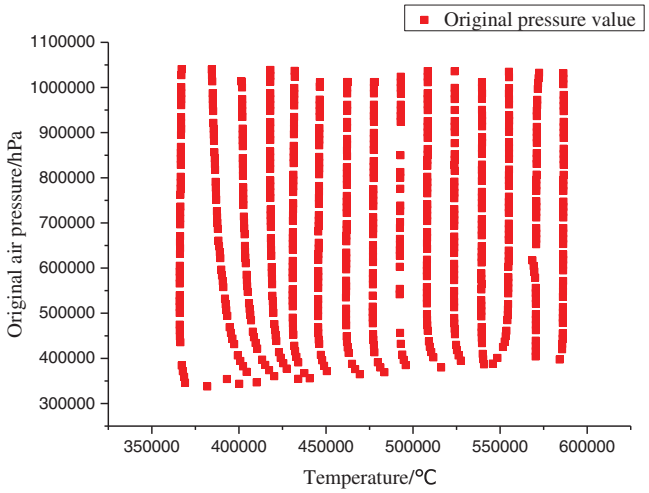

Figure 1: The relationship between temperature and air pressure

The pressure sensor of the sounding instrument is an independent module, so the calibration of the pressure sensor is also carried out in an independent way. The whole data acquisition system of the air pressure sensor includes four modules, which are composed of a constant temperature tank, a air pressure controller, and a self-made air pressure detection device. We show the flow chart of the error correction process in Fig. 2.

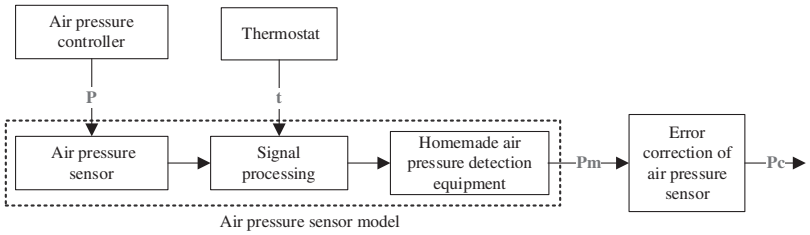

Figure 2: Error correction principle framework of the air pressure sensor

Suppose the input and output model of the air pressure sensor can be expressed as:

$$\mathrm{Pm} = f(P, t) \tag{1}$$

where P is the standard air pressure value applied by the pressure controller under the sealed container to the air pressure sensor [6], t is the temperature value at the calibration time, Pm is the real measured air pressure value obtained by the air pressure sensor with the help of self-made air pressure detection equipment. The setting of the P value is 5 hPa~1100 hPa and monotonically increasing. If the air pressure sensor model and the error correction model are reciprocal, the output of the error corrected air pressure model, that is, the true air pressure value is Pc, can be expressed as:

$$\mathrm{Pc} = \mathrm{P} = f^{-1}(Pm, t) \tag{2}$$

The essence of air pressure sensor error correction is to realize that Pm is infinitely close to P, and Pc is the value corrected by the model, so that the ideal input and output characteristic curve can be obtained [7].

2.2 Air Pressure Sensor DF-RBF Calibration Model

2.2.1 Design of the Decomposition Stage Model

Here we analyze the relationship between the input standard air pressure values and the output original air pressure values from the standard air pressure sensor input, as shown in Fig. 3. It can be seen that the input and output of the air pressure sensor follows a linear relationship and each characteristic curve can be expressed as:

$$y = kx - e \tag{3}$$

In Eq. (3), y is the standard air pressure value, x is the original air pressure value, the original pressure value is the undecrypted measured pressure value. After decryption, the value of the slope k is infinitely close to 1, and e is the error between the measured values and the standard values. According to the data collected in batches, the measured pressure value is greater than the standard pressure value, so the error value E needs to be subtracted. After that, by analyzing the distribution state of the scatter diagram between the input standard air pressure value and the output measured air pressure value, as shown in Fig. 4. It can be found that the standard pressure value and the error at different temperature points follow a certain linear relationship. This relationship can be expressed mathematically as a polynomial form, using polyfit in numpy for fitting [8]. R2 is used to evaluate the fitting degree of the model. The value of R2 is [0,1]. The closer it is to 1, the higher the fitting degree will be. It is generally considered that the model fitting

degree above 0.8 is good, while the model fitting degree above 0.9 is excellent [9]. We adopt the optimal order of this polynomial as 2 to avoid over-fitting or under-fitting [10]. In this way, the relationship between the standard pressure value and the error at each temperature point can be expressed as:

$$e = ay^2 + by + c \tag{4}$$

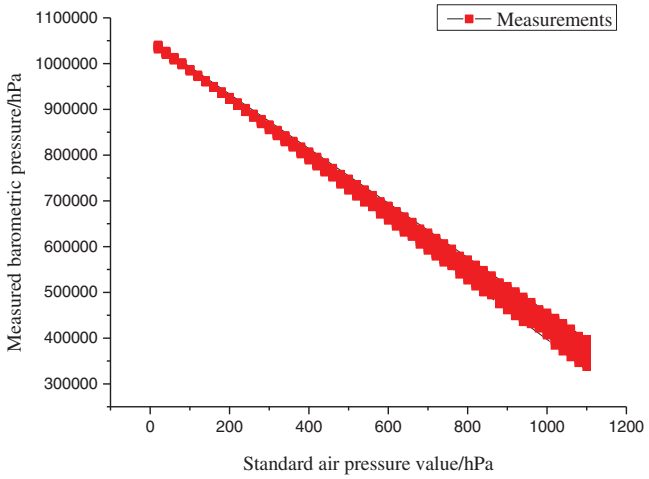

Figure 3: The characteristic curve between the standard pressure value of the pressure sensor and the measured pressure value

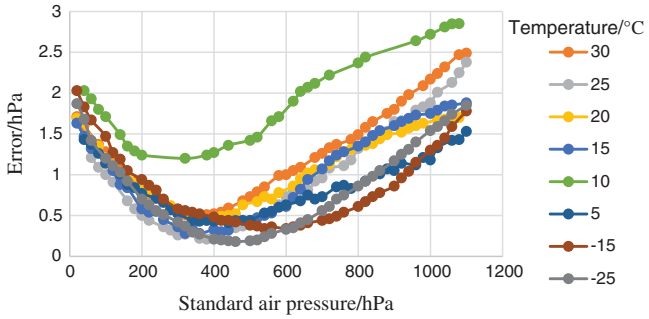

Figure 4: The linear relationship between the standard pressure and the error of 8 sets of sampled data

The y in Eq. (4) is the standard air pressure values. The detailed parameters at different temperature points fitted by polyfit are shown in Tab. 1. The training set at different temperature points dicarboxylic polynomial coefficients a, b, c values. We can observe that the number of training sets is reduced too much compared to directly using the RBF model while the training time is also reduced.

Once we determine the binomial coefficients a, b, and c, we can estimate the error corresponding by the input standard air pressure value. Then we can estimate the final Y value by combining the estimated error and the measured pressure value.

The values of R2 in Tab. 1 further elucidate that the curve fitting parameters are reliable. It can be used to predict other temperatures binomial of a, b, c coefficients. According to the input of the different temperature, each coefficient also produces corresponding change with the temperature fluctuation [11]. In the following, we will discuss how to accurately get each temperature point respectively and between a, b, c relation curve line.

Table 1: Binomial coefficients at different temperature points fitted by polyfit

Temperature (°C)	a	b	c	R^2
30	4.34E-06	–3.59E-03	1.4722	0.93
25	4.23E-06	–3.33E-03	1.0903	0.94
20	3.30E-06	–2.92E-03	1.3482	0.92
15	4.17E-06	–3.62E-03	1.3153	0.94
10	2.64E-06	–1.60E-03	1.7295	0.91
5	3.27E-06	–3.34E-03	1.3732	0.94
−15	5.15E-06	–5.81E-03	1.9580	0.97
−25	5.45E-06	–5.58E-03	1.6905	0.95

2.2.2 Comparative Study of Models in the Fitting Stage

According to binomial parameters at different temperature points of the fitting problem. Using two data fitting methods, BP neural network and RBF neural network, which are mature and widely used in existing works [12]. The binomial parameters a, b, and c listed in Tab. 1 are fed into the BP neural network and RBF neural network for target training. The input sample is the corresponding temperature. Finally, two kinds of neural networks are compared and analyzed in binomial parameter fitting, and the test result is shown in Fig. 5. It can be seen that the RBF network is better than the BP network in fitting the a, b and c coefficients at different temperatures.

3 Results

Fig. 6 shows the characteristic surface grid diagram when the pressure sensor is not calibrated [13,14]. It can be seen that the characteristic surface is distorted due to the error of the pressure sensor, resulting in the reduction of measurement accuracy.

After calibration of the measurement data collected by the air pressure sensor through the DF-RBF network model prtoposed in this paper, its characteristic surface is shown in Fig. 7. By comparing Figs. 6 and 7, it can be seen that the characteristic surface after using model calibration is smoother, which effectively reduces the error of the air pressure sensor and improves the measurement accuracy [15].

Through the characteristic surface grid graph, we conclude that the DF-RBF network model can reduce the measurement error of the air pressure sensor. To better display the calibrated air pressure value and deviation of the DF-RBF model [16], the deviation [17] is shown in Eq. (5), we choose different Temperature points and different barometric pressure values as the test set data for model verification, and some of the test results are shown in Tab. 2.

$$\text{Deviation} = (\text{calibrated air pressure value} - \text{standard air pressure value}) / \text{standard air pressure value} \quad (5)$$

It can be seen from Tab. 2 that the deviation degree after calibration is no more than 0.1%, which confirms the superiority of this model for the error calibration of the air pressure sensor.

In order to clearly observe the excellent characteristics of this model and conventional BP and RBF network models [18], we also tested two traditional models. To keep the sample data unchanged, we use Pm and t as training samples, P as the training target, and train through BP and RBF networks respectively. We obtain respective network model weights and thresholds [19], according to the trained network for new sample prediction. In Fig. 8, we represent these two methods as “BP (convention)” and “RBF (convention)”.

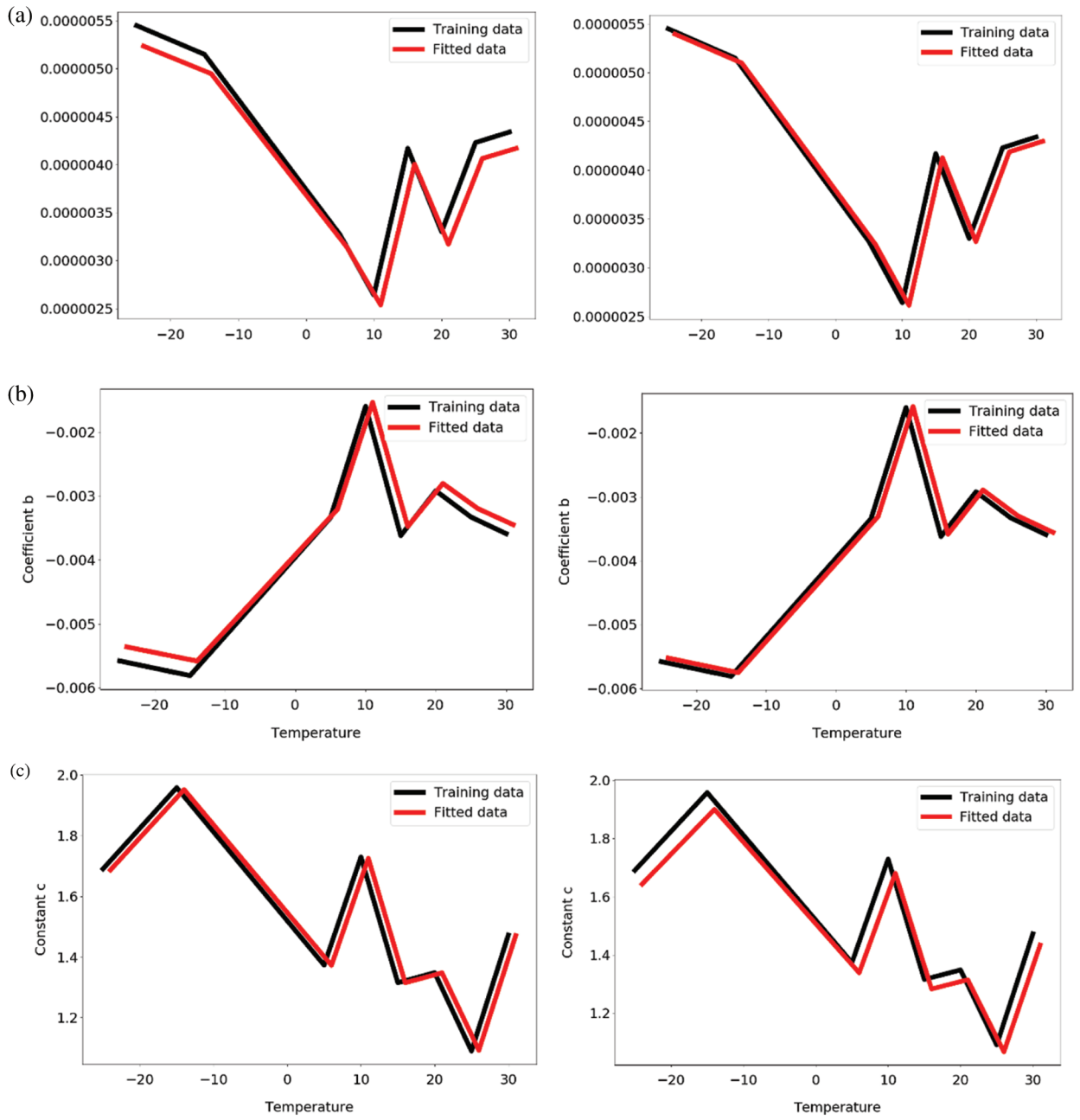

Figure 5: Comparison of BP and RBF network training data and fitted data (a) BP neural network fitting parameters a (left), RBF neural network fitting parameters a (right), (b) BP neural network fitting parameters b (left), RBF neural network fitting parameters b (right), (c) BP neural network fitting parameter c (left), RBF neural network fitting parameter c (right)

Fig. 8 can be seen, the error of the DF-RBF models as compared to conventional based RBF and BP network model [20,21] of the error value is small, the deviations are also less than 0.1%, and therefore, use of DF-RBF network model correction pressure sensor The error is feasible.

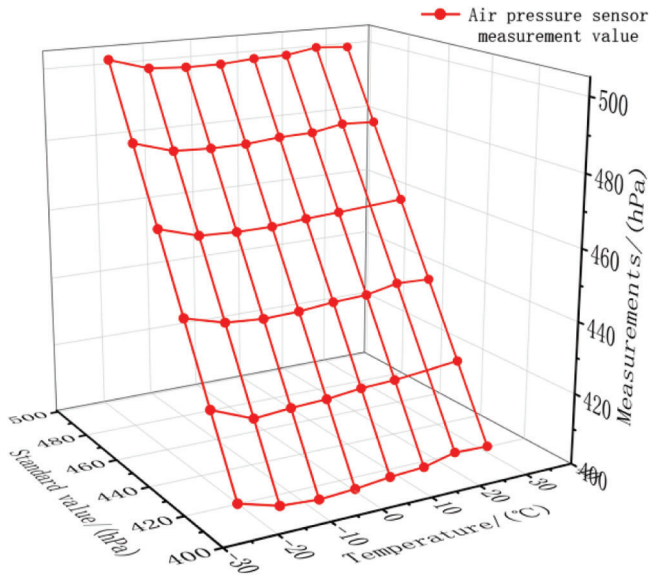

Figure 6: Uncalibrated feature surface grid

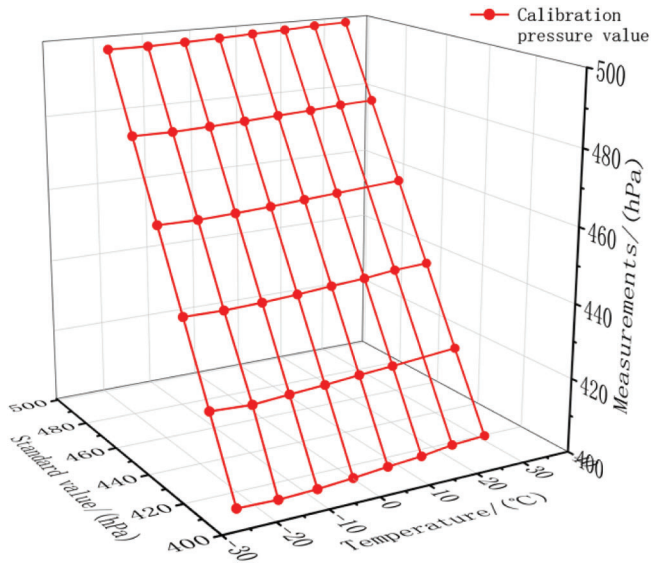

Figure 7: Characteristic surface mesh after calibration

Table 2: Test set calibration accuracy table

Standard pressure /hPa	Air pressure before calibration/hPa	Air pressure after calibration/hPa	Deviation /%
1100	1102.27	1100.25	0.023
1000	1001.53	1000.68	0.068
900	900.97	900.24	0.027
800	801.08	800.66	0.082

(Continued)

Table 2 (continued)

Standard pressure /hPa	Air pressure before calibration/hPa	Air pressure after calibration/hPa	Deviation /%
700	700.56	700.16	0.023
600	600.4	600.6	0.100
500	500.50	500.22	0.044
400	400.77	400.29	0.073
300	300.98	300.14	0.047
200	201.17	200.03	0.015
100	101.5	100.46	0.460
5	5.59	5.01	0.200

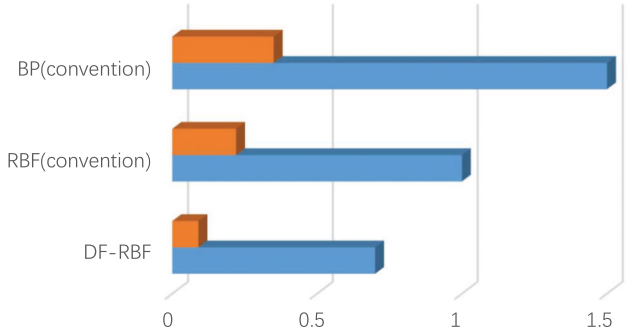

Figure 8: Test performance comparison of different algorithms

4 Conclusions

In this paper, we aim to address the imperfection of air pressure measurement. First, we analyze the distribution state of the scatter diagram between the input standard pressure value and the output measured pressure value. We construct an analytical formula of the function between the error and the temperature, and calculate the parameters of the analytical formula. We then decompose the detection problem and use the RBF network to fit the relevant parameters of the analytical formula. By combining the estimated error and the measured data we obtain the calibrated pressure value. This proposed decomposition and calibration model has been shown to enhance the high measurement accuracy meteorological instruments, reduce the need for large training sets, and reduce the training time. The final experimental results show that the error is reduced from the original 1.5 hPa to 0.7 hPa, which reduces the measurement error by 53.33%. Hence, we anticipate the proposed method to be a feasible new method for barometric sensor calibration.

Acknowledgement: First of all, I would like to thank my supervisor, Ms. Liu Pengyu. Ms. Liu made instructive comments and recommendations on the research direction of my thesis. During the process of writing the thesis, she gave timely and careful guidance on the difficulties and doubts I encountered, and put forward many useful suggestions. At the same time, I would also like to thank the students in the Multimedia Information Processing Laboratory for their strong support and help in the preparation of the paper, and also thank the family for their guidance and polish in English. Finally, thank you all for your hard work. All authors have read and agreed to the published version of the manuscript.

Funding Statement: This paper is supported by the following funds: National Key R&D Program of China (2018YFF01010100), National natural science foundation of China (61672064), Basic Research Program of Qinghai Province under Grants No. 2020-ZJ-709 and Advanced information network Beijing laboratory (PXM2019_014204_5000 29).

Conflicts of Interest: The authors declare that they have no conflicts of interest to report regarding the present study.

References

[1] X. J. Peng, *Research on the Calibration and Target Tracking Algorithm of the Pressure Sensor of the High-precision Inspection System*. Vol. 21. Hubei: Huazhong University of Science and Technology, pp. 342–353, 2015.

[2] D. M. Tan and G. M. He, "Research and technical scheme of inspection system model," *System Construction*, vol. 52, no. 4, pp. 17–20, 2003.

[3] H. H. Chang and Y. K. Chen, "Neuro-genetic approach to optimize parameter design of dynamic multiresponse experiments," *Applied Soft Computing*, vol. 32, no. 6, pp. 436–442, 2011.

[4] W. Fang, L. Pang and W. Yi, "Survey on the application of deep reinforcement learning in image processing," *Journal on Artificial Intelligence*, vol. 2, no. 1, pp. 39–58, 2020.

[5] F. Guo, C. Guo and Y. Wang, "Research on nonlinear correction of pressure sensor based on MPSO-SVM," *Chinese Journal of Sensors & Actuators*, vol. 24, no. 3, pp. 188–192, 2012.

[6] C. Nello and S. T. John, *An Introduction to Support Vector Machines and Other Kernel-based Learning Methods*. Vol. 54. Beijing: Tsinghua Publishing House of Electronics Industry, pp. 21–39, 2006.

[7] A. Janarthanan and D. Kumar, "Localization based evolutionary routing (LOBER) for efficient aggregation in wireless multimedia sensor networks," *Computers Materials & Continua*, vol. 60, no. 3, pp. 895–912, 2019.

[8] G. Q. Zhu, S. R. Liu and Y. Jinshou, "Support vector machine and its application in function approximation," *Journal of East China University of Science and Technology, Natural Science Edition*, vol. 28, no. 5, pp. 555–559, 2002.

[9] M. T. Hagan, H. B. Demuth and M. H. Beale, *Neural Network Design*. Vol. 22. USA: PWS Publishing Company, pp. 58–105, 1996.

[10] X. Y. Peng, X. M. Mai and K. Wang, *Automatic Multi-sensor Power Line Inspection System for Large Unmanned Helicopters*. Vol. 32. Guangdong Power Grid Co., Ltd., Electric Power Research Institute, Chinese Academy of Surveying and Mapping, Beijing University of Aeronautics and Astronautics, Wuhan University, the 60th Research Institute of the General Staff of the Chinese People's Liberation Army, Guangzhou Yueneng Electric Power Technology Development Co., Ltd,, pp. 44–51, 2016.

[11] D. Gao, S. Zhang, F. Zhang, X. Fan and J. Zhang, "Maximum data generation rate routing protocol based on data flow controlling technology for rechargeable wireless sensor networks," *Computers Materials & Continua*, vol. 59, no. 2, pp. 649–667, 2019.

[12] R. L. Feng, Z. F. Wang and H. Q. Feng, "Comparative study on aerodynamic resistance prediction of low-vacuum pipeline high-speed train based on RBF and BP neural network," *Journal of Vacuum Science and Technology*, vol. 40, no. 9, pp. 827–832, 2020.

[13] W. Fang, F. Zhang, Y. Ding and J. Sheng, "A new sequential image prediction method based on LSTM and DCGAN," *Computers Materials & Continua*, vol. 64, no. 1, pp. 217–231, 2020.

[14] Z. M. Yi, Z. D. Deng and J. Z. Qin, "Sintering flue gas NOx prediction based on RBF-BP hybrid neural network," *Journal of Iron and Steel Research*, vol. 32, no. 7, pp. 639–646, 2020.

[15] Y. J. Yang, M. F. Zhang and K. Q. Liu, "Application of RBF-BP composite neural network in transformer fault diagnosis," *Information Technology and Information Technology*, vol. 32, no. 6, pp. 136–137, 2020.

[16] C. F. Xu, Y. J. Qiao and L. Jun, "Fire prediction method based on LSTM and RBF-BP deep learning model," *Journal of Qilu University of Technology*, vol. 34, no. 3, pp. 53–59, 2020.

[17] J. Y. Wang, S. Wang and C. Liu, "Temperature compensation of optical fiber current transformer based on RBF neural network," *Instrument Technology and Sensor*, vol. 41, no. 6, pp. 118–121, 2020.

[18] R. Chen and H. S. Min, "Robot inverse kinematics algorithm based on BP and RBF neural network," *Machine Tool & Hydraulics*, vol. 47, no. 23, pp. 22–27, 2019.

[19] K. Niu, Z. Zhang and P. F. Wang, "PID parameter self-tuning based on improved RBF fuzzy neural network," *Electronic Design Engineering*, vol. 28, no. 12, pp. 172–177, 2020.

[20] X. L. Mao, P. Zhang and J. H. Zhang, "Sounding humidity and solar radiation error prediction based on RBF algorithm," *Modern Electronic Technology*, vol. 43, no. 19, pp. 146–151, 2020.

[21] B. Hu and Z. Sun, "Research on time synchronization method under arbitrary network delay in wireless sensor networks," *Computers Materials & Continua*, vol. 61, no. 3, pp. 1323–1344, 2019.